A full-field reflection-mode digital gradient sensing method for measuring orthogonal slopes and curvatures of thin structures

2013 Meas. Sci. Technol. 24 025202

(http://iopscience.iop.org/0957-0233/24/2/025202)

Meas. Sci. Technol. **24** (2013) 025202 (9pp) doi:10.1088/0957-0233/24/2/025202

A full-field reflection-mode digital gradient sensing method for measuring orthogonal slopes and curvatures of thin structures

Chandru Periasamy and Hareesh V Tippur[1]

Department of Mechanical Engineering, Auburn University, Auburn, AL 36849 USA

E-mail: tippuhv@auburn.edu

Received 28 June 2012, in final form 25 September 2012
Published 9 January 2013
Online at stacks.iop.org/MST/24/025202

Abstract
A full-field optical technique capable of measuring angular deflections of light rays reflected off specularly reflective planar surfaces is developed. The method is aided by 2D digital image correlation to measure angular deflection of light rays. The principle of the method is described and the governing equations that relate light ray deflections to surface slopes are presented. The method is demonstrated by measuring the orthogonal surface slopes of a circumferentially clamped silicon wafer subjected to a central load and are shown to be in good agreement with the analytical solutions. The curvature fields are also computed by taking advantage of differentiation schemes integral to digital image correlation algorithms. The method is utilized to successfully quantify relatively small surface slopes of the order of 10^{-5} rad caused by a curing layer of spin-coated epoxy on a thin (100 μm) silicon wafer.

Keywords: optical metrology, full-field measurement, thin structures, thin films, process induced deformations, slope, curvature

(Some figures may appear in colour only in the online journal)

1. Introduction

Thin structures subjected to thermo-mechanical stresses are frequently encountered in many aerospace and electronic systems. Further, fabrication of electronic and MEMS devices often requires quantitative evaluation of substrate and thin film flatness in terms of slopes and curvatures. For example, silicon wafers that are coated/deposited with thin films introduce thermo-mechanical stresses in addition to those caused during manufacturing and service. In such situations, quantification of surface characteristics such as deflection, slope and curvature assumes importance. This is partly because mechanical stresses in thin structures can be quantified from curvatures which in turn are the first and second derivatives of slopes and deflections, respectively. However, since numerically differentiated measured quantities are prone to errors, the use of deflections to obtain stresses by performing two successive differentiations is not desirable if stresses are the primary quantities of interest. In such cases, a direct measurement of surface slopes is preferred.

Previously, both coherent and incoherent optical metrology tools such as shearing interferometry and moiré-based methods have been employed to quantify surface slopes and curvatures. Assa *et al* [1] used a shearing interferometer to obtain real-time slope fringes in thin structures. Their setup could also measure curvature fringes after performing spatial filtering of the slope fringes. Kao and Chiang's [2] work provides a comprehensive description of various moiré methods used for contouring surface slopes and curvatures. The application of reflection moiré to dynamic vibration of plates has been investigated by Ritter [3]. These moiré methods involved superposing and/or relatively shifting gratings or images, which allowed optical differentiation of the displacement or slope fields. The coherent gradient sensing

[1] Author to whom any correspondence should be addressed.

(CGS) [4] technique was adopted by Lee *et al* [5] and Park *et al* [6] to quantify curvatures in thin silicon wafers coated with a thin metallic film. Tippur [7] presented a method, also using reflection-mode CGS, but capable of simultaneously measuring slope as well as curvature fringes in thin silicon wafers subjected to mechanical loading. More recently, Huang *et al* [8] devised an apparatus that measures curvatures by quantifying the change in separation distances between multiple parallel laser beams reflecting off thin metallic films subjected to rapid thermal processing.

In addition to the real-time, single exposure methods such as the ones above, double exposure methods for specularly reflective [9, 10] and diffusely reflective [11, 12] surfaces have also been developed by various researchers. These techniques are either based on the interference of diffracted light passing through or reflected off an object, or use the moiré phenomenon. Often, these methods require Ronchi rulings or grid patterns, and in some cases need monochromatic light [3]. Recently, Periasamy and Tippur [13, 14] have developed a transmission-mode digital gradient sensing (DGS) method that is capable of measuring angular deflections of light rays passing through non-uniformly stressed transparent planar objects. The setup used for transmission-mode DGS[2] can be modified to measure angular deflections of light rays reflected off an optically reflective surface. This reflection-mode DGS could be a preferred method over the current techniques for surface slope measurements, as it has advantages such as relatively simple experimental setup, inexpensive optical components and digital measurements. The prevalence of digital image correlation as a popular optical metrology tool, its ability to simultaneously measure orthogonal components of displacements, and the availability of several commercial image analysis software tools to measure displacements as well as their derivatives all make reflection-mode DGS for slope and curvature measurement attractive. By using elasticity theories, the curvatures can be further used to determine stresses in case of thin structures or films.

In the following, the experimental details and governing equations of the DGS method in reflection mode are described. The feasibility of the method to measure slopes and curvatures of thin structures is then demonstrated by studying the case of a thin edge-clamped circular plate (reflective silicon wafer) subjected to a central deflection. The measurements—slopes and curvatures—are examined relative to the theoretical counterparts based on small-deflection analysis. Finally, the DGS method is used to visualize the evolution of surface slopes *in situ* as a thin spin-coated epoxy layer is allowed to polymerize on a thin silicon wafer to show the applicability of the method to the microelectronic industry.

2. Experimental details

The schematic of the experimental setup to measure surface slopes of reflective planar objects using the reflection-mode DGS method is shown in figure 1. It consists of a digital imaging device, a beam splitter, a specularly reflective thin planar specimen and a planar speckle target. The speckle target plate is typically coated with alternate mists of black and white paints to create random speckles. The target is uniformly illuminated using two ordinary broad-band white light sources (lamps). The digital camera is fitted with a long focal length lens and/or an extension tube. The beam splitter is placed in between the specimen and the target, and is oriented at 45° to the optical axis of the camera. The camera is then focused on the target plane via the reflective surface of the specimen and through the beam splitter. Deflection of light rays from a reflective surface due to non-uniform deformations is caused by the out-of-plane displacements. A light ray that is normally incident on a specularly reflective planar surface will result in a reflected ray that is collinear with the incident ray. However, when the specimen is subjected to out-of-plane displacements, the reflected ray corresponding to the initially normal incident ray will make an angle with the local normal to the deformed surface. This angular deflection can be quantified using DGS as surface slopes.

For the sake of simplicity of analysis, consider angular deflections of light rays to occur in the plane of paper. Let (x, y) and (x_0, y_0) be the in-plane coordinates of the specimen and target planes, respectively, as shown in figure 2. Let a point

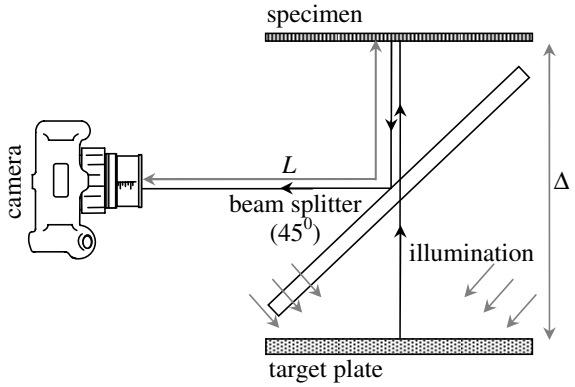

Figure 1. Schematic of DGS experimental setup in reflection.

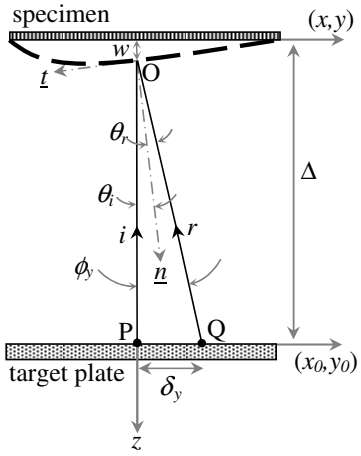

Figure 2. Details of the optical path between the specimen and target (without beam splitter for clarity); n and t denote unit vectors normal to and tangential to the specimen surface and ($\delta_{x,y}$, $w \ll \Delta$).

[2] It should be emphasized that the angular deflections produced in transmission mode are based on elasto-optic effects exhibited by phase objects subjected to load. That is, changes in thickness and refractive index deflect a ray of light propagating through a phase object.

P on the target plane be initially in focus when the specimen is planar and undeformed. In this condition, the incident (i) and reflected (r) rays will be collinear and parallel to the optical axis. Now, when the specimen undergoes out-of-plane deformation, a neighboring point Q comes into focus. Let OQ make an angle $\phi_{x,y}$ (the notation $\phi_{x,y}$ is used to denote ϕ_x or ϕ_y) relative to OP in the undeformed state. Note that in figure 2, $\phi_{x,y} = \theta_i + \theta_r$ with $\theta_i = \theta_r$ and n denotes the unit normal to the object surface at O. If the distance $\delta_{x,y}$ can be measured, and the gap between the specimen plane and the target, Δ, is known, the local surface slopes can be calculated as

$$2\frac{\partial w}{\partial x} = \tan\phi_x = \frac{\delta_x}{\Delta}, \qquad 2\frac{\partial w}{\partial y} = \tan\phi_y = \frac{\delta_y}{\Delta}. \tag{1}$$

For small angular deflections ($\delta_{x,y} \ll \Delta$) this can be written as

$$2\frac{\partial w}{\partial x} \simeq \phi_x = \frac{\delta_x}{\Delta}, \qquad 2\frac{\partial w}{\partial y} \simeq \phi_y = \frac{\delta_y}{\Delta}. \tag{2}$$

The above two equations can be viewed as the governing equations for the method of reflection-mode DGS. Evidently, the method hinges on an accurate, full-field measurement of displacement components $\delta_{x,y}$. This is accomplished using 2D digital image correlation (DIC) methodology [15–17] by photographing a stochastic gray scale distribution on the target plane before and after deformation of the thin specimen. The details of the DIC approach are well known and several commercial software packages are currently available for image registration and analysis tasks and hence will not be discussed here. It is also important to recognize that equations (1) and (2) use the coordinates of the specimen plane in the analysis although measurements are performed on the target plane using DIC. This can be accounted for by performing linear mapping of coordinates between the target and specimen planes as $(x : y) = \frac{L}{L+\Delta}(x_0 : y_0)$ (see [13]).

3. Surface slopes of a silicon wafer subjected to central load

The feasibility of reflection-mode DGS method to measure surface slopes of planar reflective surfaces is demonstrated next. A schematic of the experimental setup is shown in figure 3. The specimen is a single-face polished, 280 μm thick silicon wafer of diameter 50.8 mm. The unpolished face of the wafer is glued onto a thick steel washer using epoxy adhesive. The inner and outer diameters of the washer are 25.7 and 76.2 mm, respectively. Another steel plate with a circular aperture was mounted with a micrometer (least count = 10 μm) and placed behind the silicon wafer inside a cylindrical holder. Both the steel washer (with the bonded wafer) and the steel plate (with the micrometer) were secured using a retaining ring in the cylindrical holder. The entire assembly was then placed in front of a Nikon D3100 digital SLR camera such that the reflective side of the wafer was facing the camera. The camera was fitted with an extension tube and a 70–300 mm lens. Then, a beam splitter was positioned between the wafer and the camera at an angle of 45° to the optical axis of the camera.

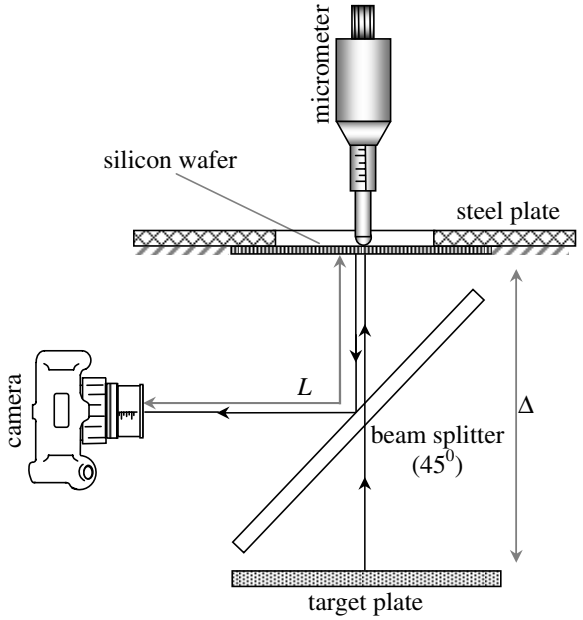

Figure 3. Schematic of the experimental setup for reflection-mode DGS to measure surface slopes of a silicon wafer subjected to central deflection.

The target plane, coated with a random black and white speckle pattern was placed parallel to the specimen at a distance of Δ = 66 mm. Now, the camera was focused on the speckle plane via the reflective face of the silicon wafer. Under no-load conditions an image was recorded which served as the reference image. Then, using the micrometer, a central out-of-plane displacement, w = 30 μm was imposed on the wafer. This deformed the wafer/specimen in the central circular region of 25.7 mm diameter, thereby distorting the speckle field relative to the undeformed counterpart (figure 4). This distorted/deformed image was recorded by the camera ($F^{\#}$ 22, 1936 × 1296 pixels, 1 pixel = 45 μm on the target plane)[3]. The two images were correlated using the method of 2D DIC and a commercial image analysis software, ARAMIS, to extract in-plane displacement fields δ_x and δ_y. During analysis, the gray scale image (8 bit) was segmented into 15 × 15 pixel non-overlapping sub-images which resulted in 78 × 92 data points in the field of view. (Other sub-image sizes ranging from 10 × 10 pixels to 30 × 30 pixels were also investigated. A 15 × 15 sub-image was found to be optimum for minimum noise in the measured values as well as minimum averaging/smoothing effects.) Once displacements for each sub-image were determined, using equation (1), the surface slopes $\frac{\partial w}{\partial x}$ and $\frac{\partial w}{\partial y}$ were calculated over the entire circular region. The results thus obtained are shown in figure 5 as solid (color) lines. The contour plots

[3] The use of a small aperture (large $F^{\#}$) for imaging speckles is helpful to achieve a good depth of field and accommodate minor misalignments in the optical components. Further, both reference and deformed states are affected equally and largely negate their influence.

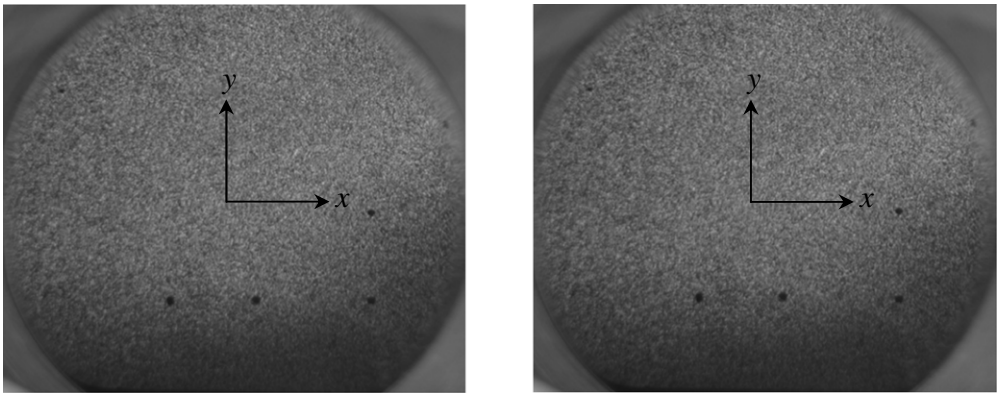

Figure 4. Reference (left) and deformed (right) images of speckles photographed off a thin silicon wafer (aperture diameter: 25.7 mm) subjected to central out-of-plane displacement of 30 μm. The speckle field distortions are small and not noticeable by the naked eye.

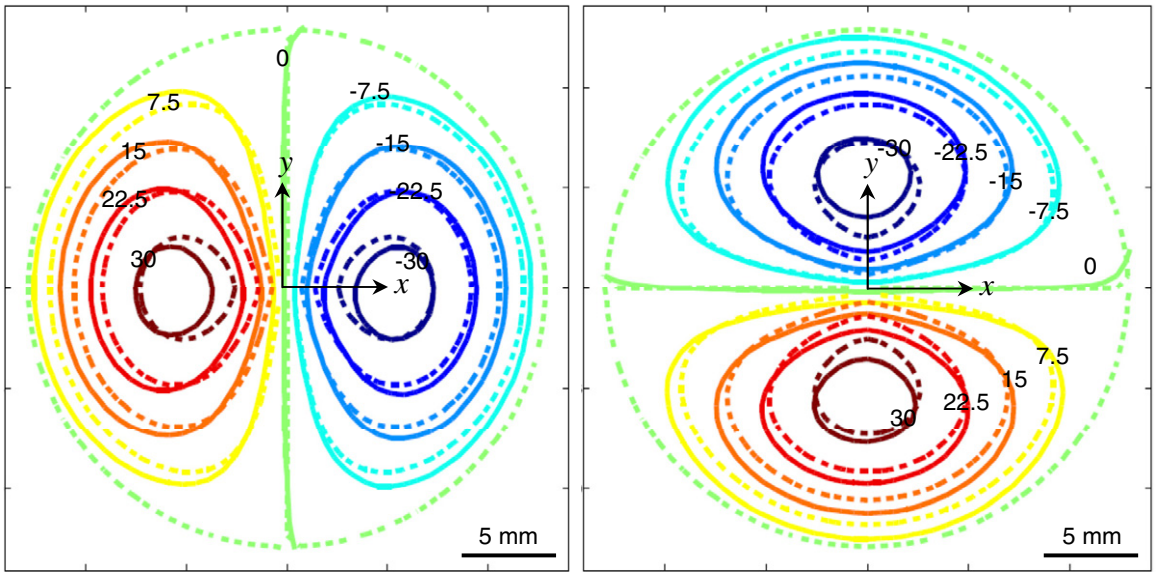

Figure 5. Comparison of experimental (solid lines) and analytical (dashed lines) contours of $\frac{\partial w}{\partial x}$ (left) and $\frac{\partial w}{\partial y}$ (right) corresponding to a circumferentially clamped silicon wafer subjected to a 30 μm central out-of-plane displacement. Contour levels are in 1×10^{-4} rad. (Color lines are used to delineate positive and negative slopes).

are shown in steps of 7.5×10^{-4} rad. (It should be noted that the smallest reliable displacement measurement for the camera parameters and the speckle pattern is approximately 3–4 μm [18] which corresponds to an angular deflection of 4×10^{-5}–6×10^{-5} rad for the chosen Δ of 66 mm.)

The plotted contours of $\frac{\partial w}{\partial x}$and $\frac{\partial w}{\partial y}$ show good symmetry about both the x- and y-axes with a higher degree of concentration of slope contours close to the concentrated load point. More importantly, it should be recognized that both these slope fields were obtained using a single pair of speckle recordings in the undeformed and deformed states of the specimen. This is unlike optical interferometric or moiré methods where two different grating orientations and/or spatial filtering operations are essential to extract orthogonal slope contours (for example, see [7] where CGS has been used to study this problem). The optical measurements from reflection-mode DGS were compared with the surface slopes for a (clamped) thin elastic plate subjected to a central deflection by a point force given by [7]

$$\frac{\partial w}{\partial x} = \frac{4xw}{R^2} \log\left(\frac{\sqrt{x^2+y^2}}{R}\right),$$
$$\frac{\partial w}{\partial y} = \frac{4yw}{R^2} \log\left(\frac{\sqrt{x^2+y^2}}{R}\right), \tag{3}$$

where w is the out-of-plane displacement and R is the clamped radius of the wafer.

The analytical results from the above equations are superimposed on the experimentally obtained contours in figure 5 as broken lines (of the same color). Excellent qualitative and quantitative agreement between the two results is clearly evident. Figure 6 shows plots of radial variations of $\frac{\partial w}{\partial x}$ and $\frac{\partial w}{\partial y}$ along the $(x, y = 0)$ and $(x = 0, y)$, respectively. Again, from the two plots, it can be seen that the experimental results generally agree with the closed form solutions very well.

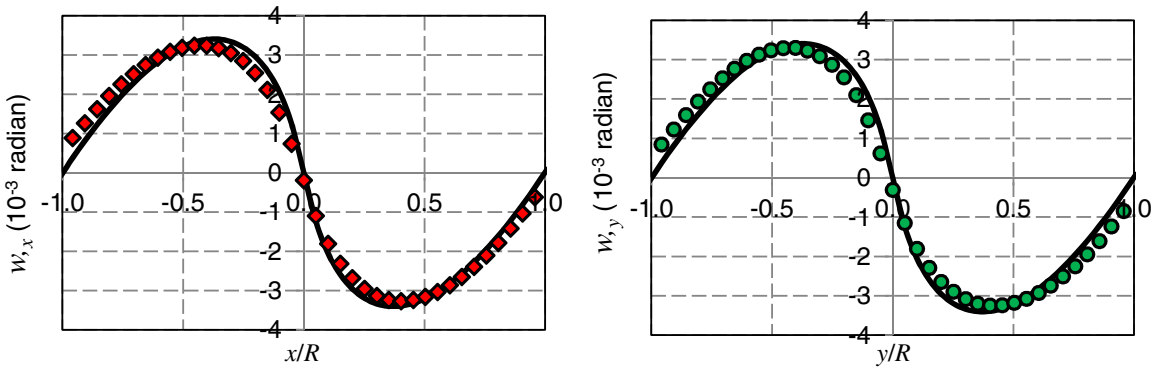

Figure 6. Comparison of analytical (solid lines) and experimental (symbols) data of $w_{,x} = \frac{\partial w}{\partial x}$ (left) along the x-axis and $w_{,y} = \frac{\partial w}{\partial y}$ (right) along the y-axis corresponding to a clamped silicon wafer subjected to a 30 μm central out-of-plane deflection.

A careful observation of figure 6 reveals that the peaks of the measured data occur slightly farther from the expected location based on analytical solution. This can be attributed to the fact that the epoxy used to glue the wafer to the steel washer is compliant to some extent, whereas the analytical solution assumes an ideally rigid clamp condition. The measured data being non-zero at $x{:}y \to R$ further substantiates this possibility. Other reasons include (a) the steeper deflections of light rays near the wafer center which cause the speckles to appear smeared in the deformed image and hence the speckle decorrelation and uncertainty in that region, (b) averaging effect due to the finite sub-image size (15 $\times$ 15 pixels) used for DIC.

3.1. Estimation of curvatures

One of the advantages of DIC analysis is its ability to provide full-field spatial derivatives of the measured (displacement) data. In reflection-mode DGS, δ_x and δ_y measurements being proportional to surface slopes, $\frac{\partial w}{\partial x}$ and $\frac{\partial w}{\partial y}$, the measurements can be differentiated once with respect to the in-plane spatial coordinates to estimate curvatures. (In elastic plate theory, curvatures can be directly related to stresses and hence will be valuable to assess thin plate/film stresses.) Most DIC software packages offer such a facility since displacement derivatives are integral to speckle/texture correlation algorithms. Exploiting this, derivatives of DGS measurements were obtained using the in-built algorithms of ARAMIS, and related to the respective curvatures as

$$2\frac{\partial^2 w}{\partial x^2} \simeq \frac{\partial}{\partial x}\left(\frac{\delta_x}{\Delta}\right), \qquad 2\frac{\partial^2 w}{\partial y^2} \simeq \frac{\partial}{\partial y}\left(\frac{\delta_y}{\Delta}\right). \tag{4}$$

For the parameters used in the DGS measurements, curvatures of the order of 10^{-4} mm^{-1} were discernible from the measurements. The contour plots of curvatures thus obtained are shown in figure 7. As expected, larger curvatures with an asymptotic trend occur close to the loading point. For comparison, the analytical curvature fields given by [7]

$$\frac{\partial^2 w}{\partial x^2} = \frac{4w}{R^2}\log\left(\frac{\sqrt{x^2+y^2}}{R}\right) + \frac{4x^2 w}{R^2(x^2+y^2)}, \qquad \frac{\partial^2 w}{\partial y^2} = \frac{4w}{R^2}\log\left(\frac{\sqrt{x^2+y^2}}{R}\right) + \frac{4y^2 w}{R^2(x^2+y^2)}, \tag{5}$$

are also superposed on the experimental contours. The measured curvature distribution is generally in good agreement, both qualitatively and quantitatively, with the predictions despite the additional numerical processing of measured slope data. The non-conformities between the measured data and analytical solutions can be partly attributed to the numerical error from the differentiation process as well as the sub-image averaging effect. Figure 8 shows plots of radial variations of $\frac{\partial^2 w}{\partial x^2}$ and $\frac{\partial^2 w}{\partial y^2}$ along the x- and y-axes. Given the fact that epoxy used to glue the wafer to the steel plate is not perfectly rigid but elastic, the agreement between the measured and analytical fields is indeed good. As noted earlier, the deviations are notably higher near the center of the plate where the surface slopes are relatively large and the numerical differentiation of slope data further exasperate the resulting curvatures.

The availability of full-field digital/numerical data also facilitates numerical differentiation of one surface slope field with respect to either of the two orthogonal coordinates. Therefore, it is possible to evaluate gradients of $\frac{\partial w}{\partial x}$ and $\frac{\partial w}{\partial y}$ with respect to the y- and x-axes to obtain twist fields, $\frac{\partial^2 w}{\partial x \partial y}$ and $\frac{\partial^2 w}{\partial y \partial x}$, respectively. The results thus obtained are shown in figure 9. As expected, the two twist fields are nearly identical qualitatively as well as quantitatively after allowing for experimental and numerical differentiation errors. The skew symmetry of the twist contours is also evident.

4. Curing-induced surface slopes of a polymer coated silicon wafer

One of the potential applications of the proposed reflection DGS methodology is to monitor the evolution of surface slopes and curvatures (and hence stresses) during deposition and curing of dissimilar material films on silicon wafers during

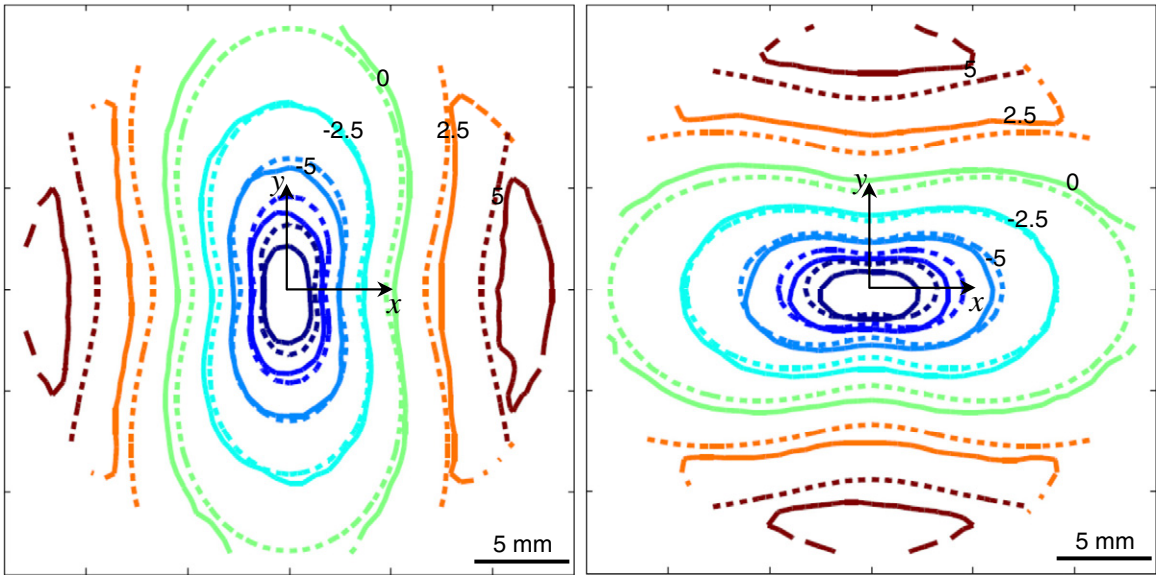

Figure 7. Comparison of experimental (solid lines) and analytical (dashed lines) contours of $\frac{\partial^2 w}{\partial x^2}$ (left) and $\frac{\partial^2 w}{\partial y^2}$ (right) corresponding to a circumferentially clamped planar silicon wafer subjected to a central 30 μm out-of-plane displacement. Contour levels are in 1×10^{-4} mm^{-1}.

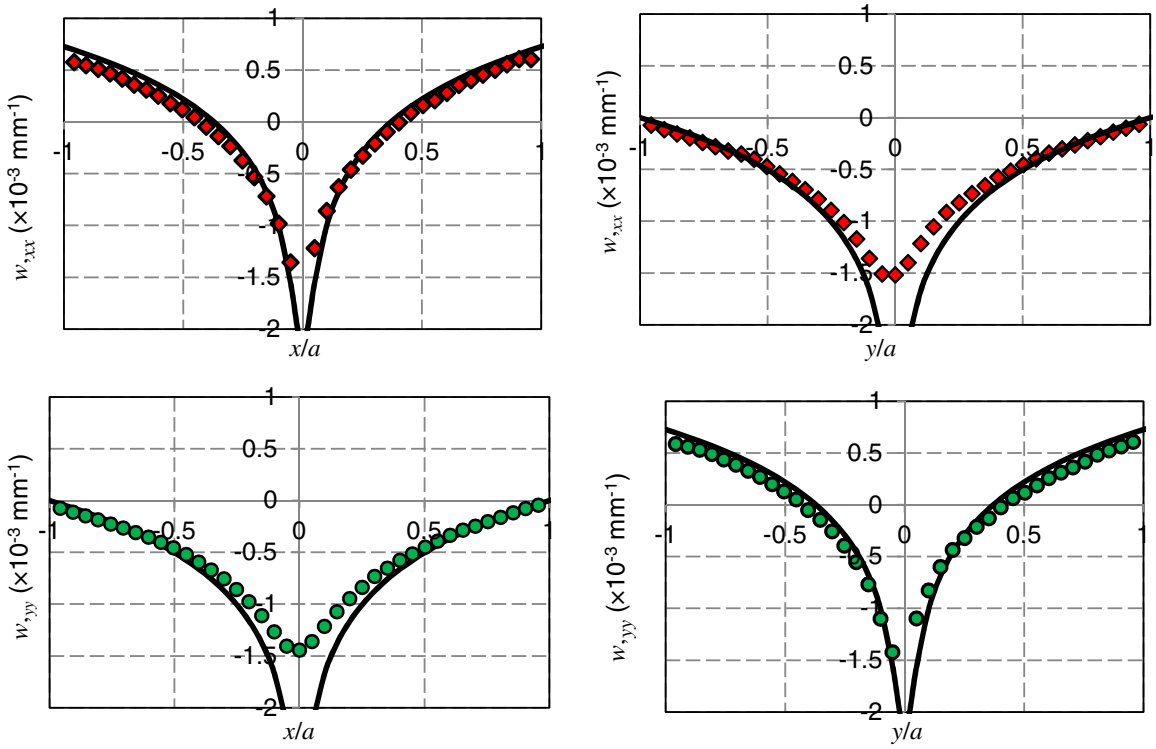

Figure 8. Comparison of analytical (solid lines) and experimental (symbols) curvatures of $w_{,xx} = \frac{\partial^2 w}{\partial x^2}$ (top) and $w_{,yy} = \frac{\partial^2 w}{\partial y^2}$ (bottom) along horizontal (left) and vertical (right) diameters corresponding to a circumferentially clamped silicon wafer subjected to a 30 μm central out-of-plane displacement.

microelectronic fabrication. To demonstrate this feasibility, an experiment in which slopes and curvatures of a thin silicon wafer, spin-coated with a layer of uncured epoxy and monitored during the initial stages of the curing process, was conducted. As evident from figure 2, by increasing the separation distance Δ between the object and target planes, the displacements (δ_x and δ_y) can be magnified using the optical arm, for the same angular deflection values. This feature is of significance in situations where very small ($<1 \times 10^{-4}$ radians) angular deflections are encountered/expected, as the resolution of DGS could be intrinsically adjusted thereby minimizing measurement errors associated with small angular deflections. Equipped with this information, a feasibility experiment to measure the small

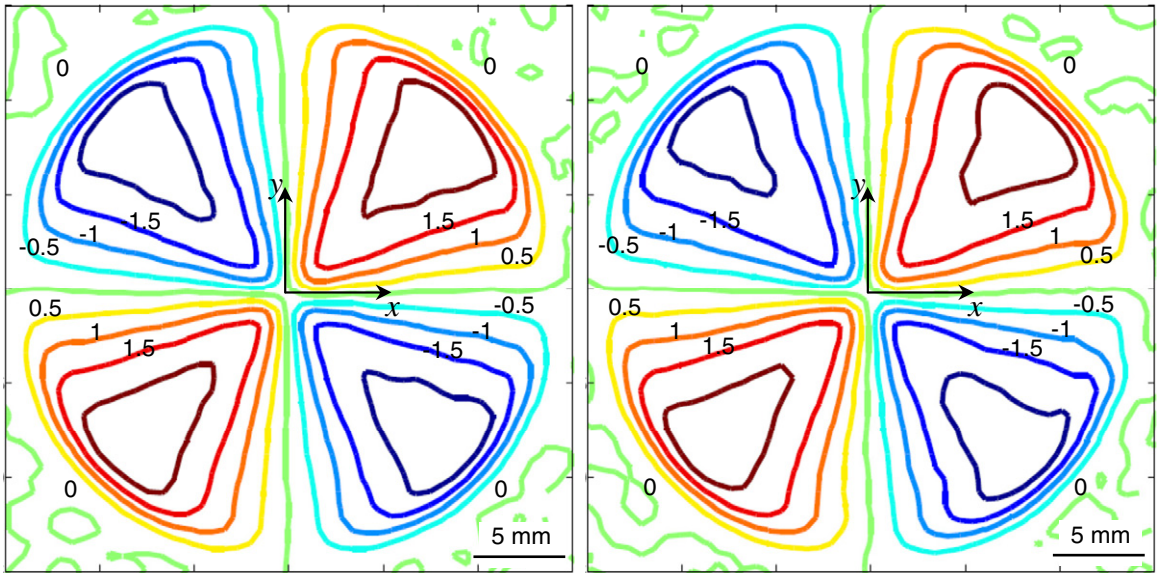

Figure 9. Contour plots of $\frac{\partial^2 w}{\partial x \partial y}$ (left) and $\frac{\partial^2 w}{\partial y \partial x}$ (right) corresponding to a circumferentially fixed silicon wafer subjected to a 30 μm central out-of-plane displacement. Contour levels are in $\times 10^{-4}$ mm^{-1}.

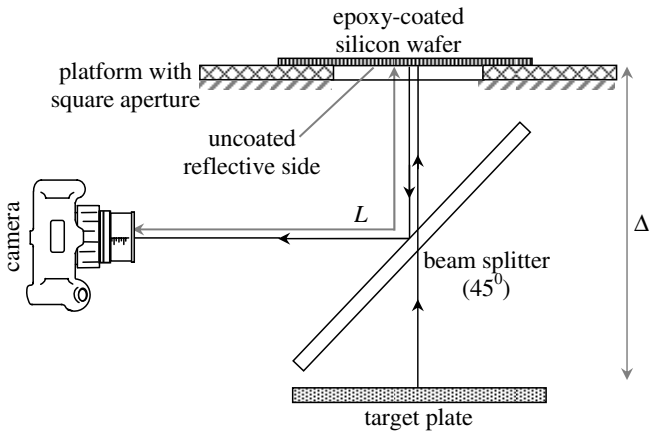

Figure 10. Schematic of the experimental setup used to measure surface slopes of a 100 μm thick silicon wafer caused by the *in situ* curing of a thin epoxy film.

surface slopes induced by *in situ* curing of a thin layer of epoxy film on one face of a thin silicon wafer was performed. A schematic of the experimental setup used is shown in figure 10. A 50.8 mm diameter, 100 μm thick double side polished silicon wafer was spin-coated on one side with 20–30 μm thick epoxy (Epothin®—a two part, low viscosity epoxy from Buehler Inc., USA; gel time ~20 min at room temperature) layer. The epoxy-coated wafer was freely rested on a rigid platform with a square clear aperture placed parallel to the tabletop. The uncoated side faced the speckle target positioned parallel to it, at a distance of $\Delta = 472$ mm (note that a large Δ is chosen since the expected deformations are relatively small in this experiment). A beam splitter was placed in-between the coated wafer and the target and oriented at 45° to the wafer surface. A Nikon D3000 DSLR camera fitted with an extension tube and a 70–300 mm focal length lens was positioned at a distance of $L = 1505$ mm from the wafer surface. Then, the camera was focused on the speckled target via the beam splitter and the silicon wafer. Then, a reference image of the speckles was recorded at time $t = 0$ min (corresponding to 10 min after the start of mixing the two-part epoxy resin and hardener).

The images were recorded through a 70–300 mm lens with $F^{\#}$ 22 aperture, and a resolution of 1936 × 1296 pixels, each pixel corresponding to 59.4 μm on the target plane. Subsequently, perturbed images of the speckles while the epoxy cured at room temperature, were recorded at every 5 min intervals for up to 1 h. The 'deformed' speckle images were then correlated with the reference image to obtain the $\frac{\partial w}{\partial x}$ and $\frac{\partial w}{\partial y}$ contours and results for a few select times are shown in figure 11. As noted earlier, the coordinates of the contour plots were corrected for perspective effect introduced by the large Δ ([13]) using coordinate mapping functions. During analyses, the recorded images were segmented into 15 × 15 non-overlapping sub-images which resulted in 75 × 98 data points at each time step.

The time-resolved contour plots in figure 11 show the evolution of surface slopes in the silicon wafer as the epoxy film cures. In the early stages of curing, the contours (t = 0–25 min) are randomly shaped and oriented, whereas subsequent contours ($t = 35$ min) reveal a definite organization in terms of shape and orientation. The increase and decrease in contour densities between $t = 35$ and 55 min is indicative of the time-dependent deformation in the wafer caused by the curing of epoxy film. There is a monotonic increase in the number of slope contours up to ~45 min of the curing cycle as the film continues to polymerize and cross-link. Subsequently, a drop in the number of contours (and the magnitude of surface slopes) is evident suggesting a degree of relaxation of the wafer from progressive warping, possibly attributed to micro-scale debonding between the wafer and the epoxy film. In this first qualitative demonstration of the curing-induced deformations, the continuous monitoring of the epoxy coated wafer was discontinued beyond the last frame in view of the demonstrative nature of the work. The slope contours at $t = 35$,

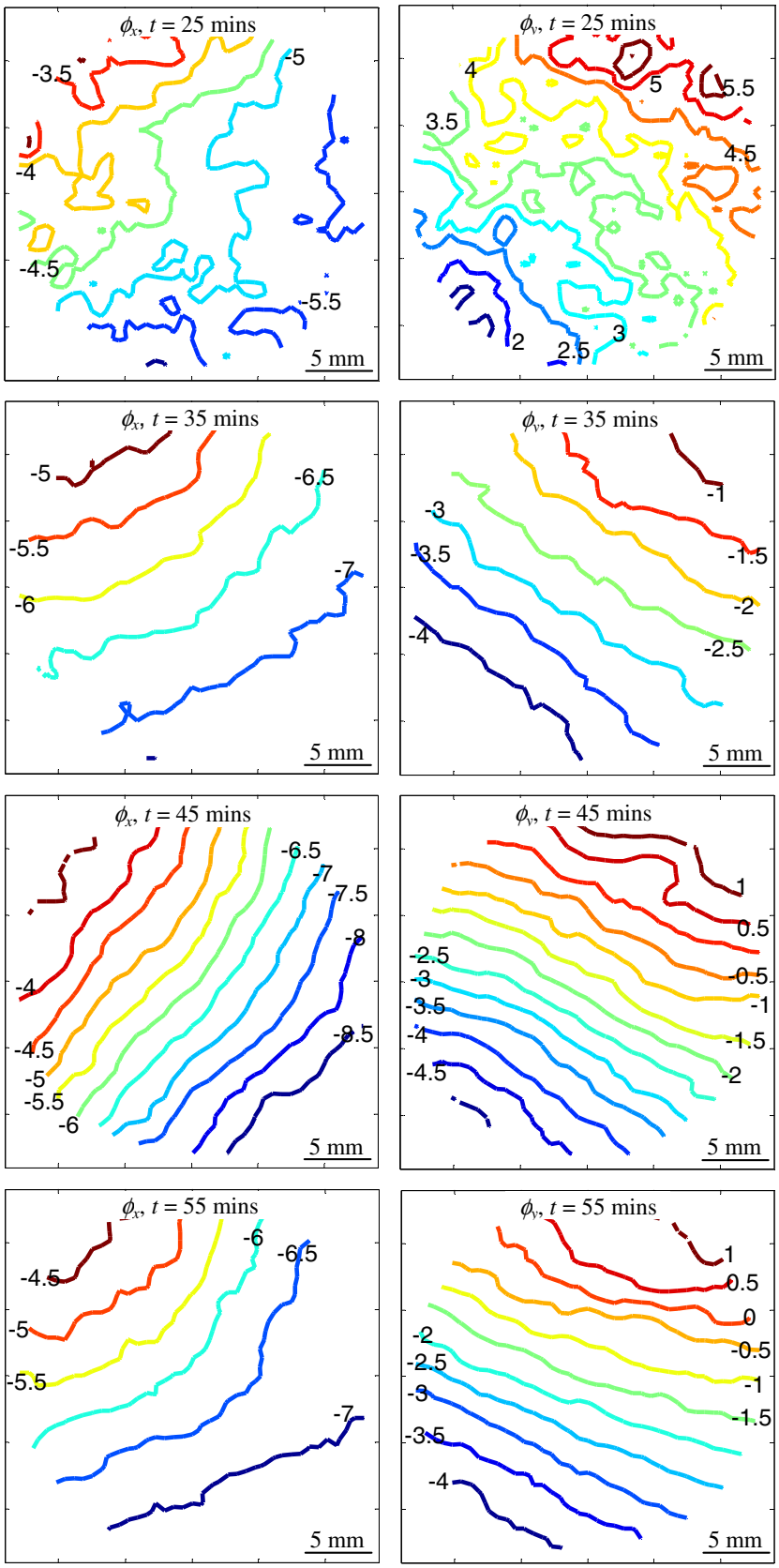

Figure 11. Evolution of orthogonal surface slopes $w_{,x}$ and $w_{,y}$ of the silicon wafer as epoxy film cures on the wafer. Contour levels are in 1×10^{-5} rad.

45 and 55 min suggest a relatively uniform deformation of the wafer as suggested by the near-parallel and uniformly spaced orthogonal slope contours. This in turn results in a relatively uniform curvature of the wafer. A more rigorous demonstration of the method spanning the entire curing cycle is planned by incorporating vibration and thermal current isolation of the setup.

5. Conclusions

A reflection-mode digital gradient sensing (DGS) technique has been demonstrated for performing non-contact measurement of angular deflections of light rays when a polished silicon wafer is subjected to out-of-plane deformation. The optical measurements were related to orthogonal surface slopes of the wafer and compared with closed form solutions for a circular thin clamped plate subjected to a central deflection by a concentrated force. Good agreement between the two is observed. The surface slope fields were also differentiated to obtain curvatures and twist of the wafer. Again, good agreement of measurements with the ones from closed form solution of the problem is observed. A feasibility experiment to monitor and quantify warpage of a thin silicon wafer due to *in situ* curing of a thin polymer layer on a silicon wafer has been demonstrated. In this demonstration, surface slopes of the order of 1×10^{-5} rad have been measured showing the potential of the method for inspection and monitoring of process-induced deformations of thin structures encountered in the microelectronics industry.

Acknowledgments

Partial support for this research through grants W911NF-12-1-0317 from the US Army Research Office and NSF CMMI-1232821 from the National Science Foundation is gratefully acknowledged.

References

[1] Assa, Betser A A and Politch J 1977 Recording slope and curvature contours of flexed plates using gratings shearing interferometer *Appl. Opt.* **16** 2504–13
[2] Kao T Y and Chiang F P 1982 Family of grating techniques of slope and curvature measurements for static and dynamic flexure of plates *Opt. Eng.* **21** 721–42
[3] Ritter R 1982 Reflection moire methods for plate bending studies *Opt. Eng.* **21** 663–71
[4] Tippur H V, Krishnaswamy S and Rosakis A J 1991 Optical mapping of crack tip deformations using the methods of transmission and reflection coherent gradient sensing - a study of crack tip K-Dominance *Int. J. Fract.* **52** 91–117
[5] Lee H, Rosakis A J and Freund L B 2001 Full-field optical measurement of curvatures in ultra-thin-film-substrate systems in the range of geometrically nonlinear deformations *J. Appl. Phys.* **89** 6116–29
[6] Park T S, Suresh S, Rosakis A J and Ryu J 2003 Measurement of full-field curvature and geometrical instability of thin film-substrate systems through CGS interferometry *J. Mech. Phys. Solids* **51** 2191–211
[7] Tippur H V 2004 Simultaneous and real-time measurement of slope and curvature fringes in thin structures using shearing interferometry *Opt. Eng.* **43** 3014–20
[8] Huang R, Taylor C A, Himmelsbach S, Ceric H and Detzel T 2010 Apparatus for measuring local stress of metallic films using an array of parallel laser beams during rapid thermal processing *Meas. Sci. Technol.* **21** 055702
[9] Patorski K 1986 Generation of the derivative of out-of-plane displacements using conjugate shear and moire interferometry *Appl. Opt.* **25** 3146–51
[10] Heise U 1966 A moire method for measuring plate curvature *Exp. Mech.* **7** 47–48
[11] Chiang F P and Juang R M 1976 Laser speckle interferometry for plate bending problems *Appl. Opt.* **15** 2199–204
[12] Hung Y Y and Durelli A J 1978 Simultaneous measurement of three displacement derivatives using a multiple image-shearing interferometric camera *J. Strain Anal.* **14** 81–8
[13] Periasamy C and Tippur H V 2012 A full-field digital gradient sensing method for evaluating stress gradients in transparent solids *Appl. Opt.* **51** 2088–97
[14] Periasamy C and Tippur H V 2012 Measurement of orthogonal stress gradients due to impact load on a transparent sheet using digital gradient sensing method *Exp. Mech.* online, doi:10.1007/s11340-012-9653-x
[15] Chen D J, Chiang F P, Tan Y S and Don H S 1993 Digital speckle-displacement measurement using a complex spectrum method *Appl. Opt.* **32** 1839–49
[16] Chu T C, Ranson W F, Sutton M A and Peters W H 1985 Application of digital image correlation techniques to experimental mechanics *Exp. Mech.* **25** 232–44
[17] Sutton M A, Orteu U and Schreier H 2009 *Image Correlation for Shape, Motion and Deformation Measurements* (Berlin: Springer)
[18] Kirugulige M S, Tippur H V and Denney T S 2007 Measurement of transient deformations using digital image correlation method and high-speed photography: application to dynamic fracture *Appl. Opt.* **46** 5083–96